Neuron, Vol. 41, 313–319, February 19, 2004, Copyright ©2004 by Cell Press

Report

Three-Dimensional Structure of I_{to}: Kv4.2-KChIP2 Ion Channels by Electron Microscopy at 21 Å Resolution

Leo A. Kim,[1] Johannes Furst,[2,3] David Gutierrez,[2] Margaret H. Butler,[1] Shuhua Xu,[1] Steve A.N. Goldstein,[1,*] and Nikolaus Grigorieff[2]

[1]Department of Pediatrics
Department of Cellular and Molecular Physiology
Boyer Center for Molecular Medicine
Yale University School of Medicine
295 Congress Avenue
New Haven, Connecticut 06535

[2]Howard Hughes Medical Institute
Department of Biochemistry
Rosenstiel Basic Medical Sciences Research Center
Brandeis University
415 South Street
Waltham, Massachusetts 02454

Summary

Regulatory KChIP2 subunits assemble with pore-forming Kv4.2 subunits in 4:4 complexes to produce native voltage-gated potassium (Kv) channels like cardiac I_{to} and neuronal I_A subtypes. Here, negative stain electron microscopy (EM) and single particle averaging reveal KChIP2 to create a novel ~35 × 115 × 115 Å, intracellular fenestrated rotunda: four peripheral columns that extend down from the membrane-embedded portion of the channel to enclose the Kv4.2 "hanging gondola" (a platform held beneath the transmembrane conduction pore by four internal columns). To reach the pore from the cytosol, ions traverse one of four external fenestrae to enter the rotundal vestibule and then cross one of four internal windows in the gondola.

Introduction

Accessory (β) subunits are a fundamental feature of potassium channels in animals that determine channel location, abundance, sensitivity to stimulation, and pharmacology (Abbott and Goldstein, 1998; Shibata et al., 2003). Despite their importance, the structural basis for accessory subunit function remains to be elucidated. High-resolution structures of pore-forming potassium channel α subunits, without accessory subunits, have revealed how four α subunits create a central, membrane-spanning, ion conduction pathway and offered clues to mechanisms by which stimuli induce pores to open and close (Cushman et al., 2000; Zhou et al., 2001a, 2001b; Jiang et al., 2002, 2003; Kuo et al., 2003). Crystal structures have also been solved for two β subunits in isolation: the neuronal calcium sensing (NCS) protein Frequenin (Bourne et al., 2001) and Kvβ2 (revealing it to be a tetrameric nicotinamide oxidoreductase) (Gulbis et al., 1999). Furthermore, Kvβ2 has been visualized in a 4:4 complex with T1, a cytoplasmic domain of ~100 residues that precedes the first membrane span in Kv1 and Kv4 family α subunits and prevents assembly of α subunits from different Kv families (Gulbis et al., 2000). Four α subunits provide four T1 domains to generate an intracellular "hanging gondola" (Kreusch et al., 1998; Kobertz et al., 2000; Sokolova et al., 2001; Zhou et al., 2001a): four columns that extend below the transmembrane pore to a central platform. The gondola has four lateral windows that ions (and inactivation particles) traverse to reach the pore, and these remain unobstructed by four Kvβ2 subunits that dock beneath the platform in the crystal structure (Gulbis et al., 2000). Supporting this arrangement in complete channels, EM and single particle reconstitution of Shaker Kv channels without accessory subunits reveal a four-windowed gondola (Sokolova et al., 2001), and native Kv1 channels (subtypes 1.1, 1.2, 1.4, and 1.6) copurified from rat brain with Kvβ2 via dendrotoxin binding show density below the gondola consistent with Kvβ2 tetramers (Orlova et al., 2003).

To further understand the structure and function of potassium channels with accessory subunits, we chose to study Kv4.2-KChIP2 channels by EM for two reasons. First, to function correctly in the heart and nervous system, Kv4 subunits assemble in stable fashion with intracellular NCS proteins like KChIP2 or Frequenin (Nakamura et al., 2001; Guo et al., 2002); thus, co-assembly alters channel trafficking, surface half-life, voltage dependence, rate of opening, inactivation and recovery from inactivation, and kinase regulation (An et al., 2000) and explains the character and distribution of I_{to} in the heart (Kuo et al., 2001; Rosati et al., 2001). Second, as demonstrated in a companion report (Kim et al., 2003), appropriate amounts of intact Kv4.2-KChIP2 complexes (tens of pmol) can be purified and shown to be of high purity and functional quality. This is achieved with a variant of Kv4.2 (Kv4.2*) that is sensitive to nanomolar levels of charybdotoxin (CTX) and bears an epitope tag to allow affinity purification from mammalian tissue culture cells under mild conditions. Integrity of purified complexes can be confirmed because proper α subunit folding and tetrameric assembly is required to bind CTX in the pore. Although channels with only Kv4.2 subunits could not be isolated (perhaps, because KChIPs increase expression level and solubility in nonionic detergent [Shibata et al., 2003]), Kv4.2*-KChIP2 channels are readily purified in quantities sufficient to determine that they have four subunits of each type using direct amino acid analysis (Kim et al., 2003). Here, single purified Kv4.2*-KChIP2 channels were visualized by EM with contrast-enhancing negative stain in order to reconstruct a 3D structure at 21 Å resolution.

Results

Depending on their orientation, channel particles appeared square or displayed a double-layered structure

*Correspondence: steve.goldstein@yale.edu

[3]Present address: Institute of Physiology, University of Innsbruck, Fritz-Pregl-Str. 3, A-6020 Innsbruck, Austria.

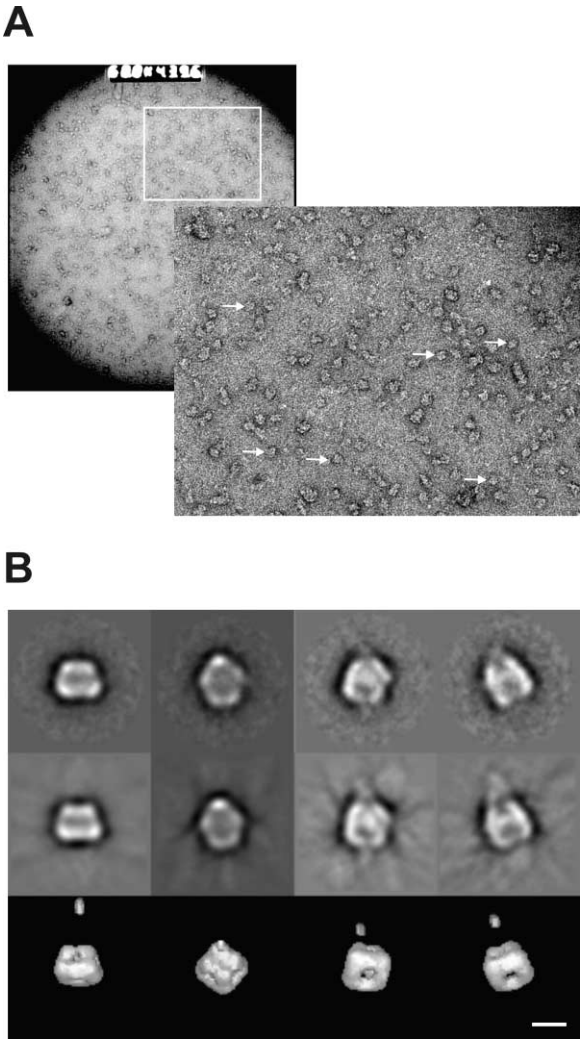

Figure 1. Electron Microscopy and IMAGIC Image Processing

(A) Purified Kv4.2*-KChIP2 complexes on carbon-coated copper grids were stained with 1% uranyl acetate and visualized by EM to obtain single particle images (arrows).

(B) Single particle images were filtered, classified, and aligned to produce class averages (top row). Surface views (bottom row) of the IMAGIC structure, with views that correspond to the class averages from the top row. Reprojections of the IMAGIC structure (middle row) for class averages in the top row. Scale bar equals 100 Å.

(Figure 1A). Particles (13,351) were manually selected and processed using IMAGIC (van Heel et al., 1996) to yield 50 classes (Figure 1B, top row, four shown). As expected, because Kv4.2* channels have four α subunits and KChIP2 is equimolar (Kim et al., 2003), unbiased class averages revealed approximate 4-fold symmetry (see Supplemental Figure S1 at http://www.neuron.org/cgi/content/full/41/4/513/DC1). Thereafter, 4-fold symmetry was imposed through five iterations of image processing by IMAGIC to produce the initial three-dimensional (3D) structure shown in four views in Figure 1B (bottom row) corresponding to four classes. Reprojections of the structure correspond closely with the class averages (Figure 1B, middle row), indicating consistency between the structure and the classes.

After initial image reconstruction with IMAGIC, each particle image was corrected for the contrast transfer function (CTF) of the electron microscope, and the *x*, *y* positions and Euler angles of the particles were further refined using FREALIGN (Grigorieff, 1998) in order to calculate an improved reference structure. A stable refined structure was produced after 15 iterations of particle parameter refinement and 3D reconstruction (Figures 2A–2E). The final distribution of Euler angles shows complete coverage of angular space, although there are some preferred orientations (Figure 2F). The final structure contained 8164 particles and was determined at an estimated resolution of 21 Å based on a Fourier shell correlation (FSC) of 0.5, calculated between two reconstructions, each derived from one half of all particles in the data set (Figure 2G).

Overall, the Kv4.2*-KChIP2 complex is $\sim$85 Å tall with two prominent domains (Figure 2A). The smaller domain is $\sim$30 $\times$ 95 $\times$ 95 Å (Figures 2B and 2C), while the larger domain is $\sim$35 $\times$ 115 $\times$ 115 Å (Figures 2B and 2E). These densities are held $\sim$20 Å apart by eight columns, four that are central and four at the channel periphery that are offset by 45° and link the smaller and larger domains (Figure 2D).

To establish the topology of the complex, a second structure was determined for a channel variant that carried a mass tag large enough to be visualized by EM at a site known to be in the cytoplasm; thereafter, a difference map with the parent structure was calculated revealing the larger domain to be intracellular (Figure 3). Thus, KChIP2 (252 residues, $\sim$28 kDa), which resides inside the cell, was enlarged by linkage in tandem with 265 residues of green fluorescent protein (GFP, $\sim$29 kDa) to produce GFP-KChIP2. Like a similar construct studied by others (Takimoto et al., 2002), GFP-KChIP2 was found to alter the biophysical function of Kv4.2* in a manner similar to wild-type KChIP2, increasing current density, decreasing inactivation rate, shifting the voltage dependence of channel activation and inactivation, and increasing the rate of recovery from inactivation (Figure 3A; Supplemental Table S1 and Supplemental Figure S2 at http://www.neuron.org/cgi/content/full/41/4/513/DC1). Also like wild-type KChIP2 (Kim et al., 2003), GFP-KChIP2 increased surface expression $\sim$2- to 3-fold as judged by ^{3}H-CTX binding (3.4 $\pm$ 0.6 pmol/plate, n = 3), permitted ready purification of Kv4.2*-GFP-KChIP2 channels (Figure 3B), and assembled with Kv4.2* in 4:4 complexes as assessed by amino acid analysis using the strategy detailed in a companion report (Kim et al., 2003; Supplemental Table S2).

An independent 3D structure calculated for Kv4.2*-GFP-KChIP2 complexes by selection of 5553 particles and analysis with IMAGIC and FREALIGN revealed the new complex to be taller, $\sim$110 Å high (Figure 3C, pale blue, 4449 particles were included in the structure). Although fewer features were resolved (perhaps due to effects of flexible GFP tags on image alignment or stain artifacts, see below), the parent and GFP-bearing structures were readily aligned using the four peripheral columns (Figure 3C, Experimental Procedures). A difference map (Figure 3D, green) shows a significant positive peak next to the large domain, corresponding in size to the four GFP appendages (based on the GFP crystal structure, Figure 3C, inset) and thereby indicating that

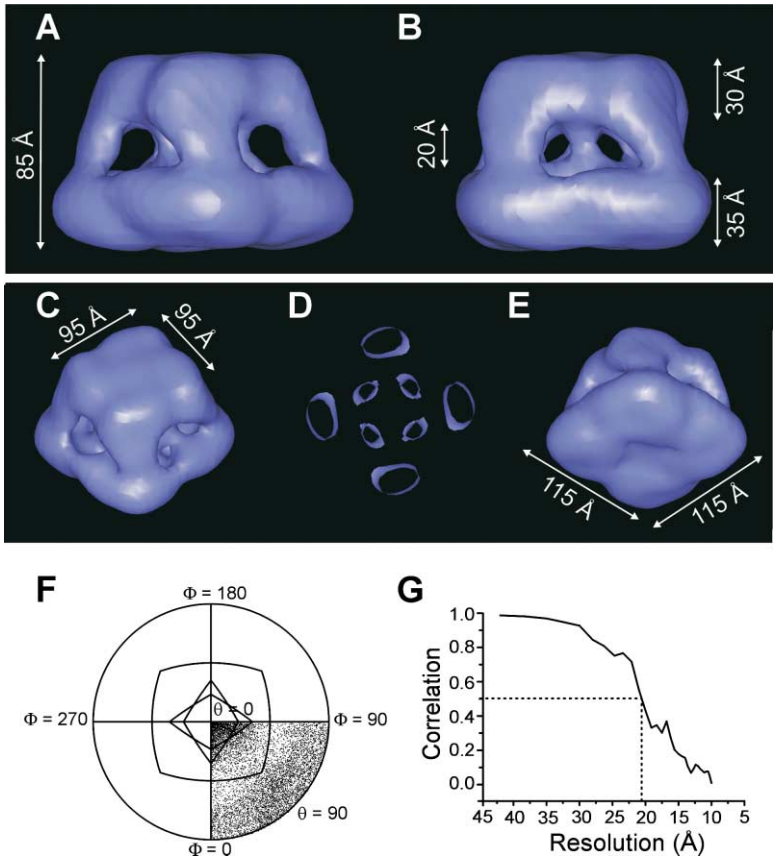

Figure 2. Kv4.2*-KChIP2 Channel Structure after Refinement with FREALIGN

(A) Side view, showing the structure is ~85 Å high with a small upper domain and large lower domain separated by columns.

(B) Side view rotated by 45° from (A) along the central axis of symmetry. The smaller domain is ~30 Å high, the larger domain ~35 Å high, and the domains are separated by ~20 Å. One of four windows between the peripheral columns is seen in front.

(C) Oblique top view, showing the smaller domain to be ~95 Å^2. The peripheral columns link the small and large domains at their corners.

(D) Cross-section through the 20 Å space between the major domains, showing four internal and four external columns offset by 45°.

(E) Oblique bottom view, showing the larger domain to be ~115 Å^2.

(F) Distribution of Euler angles for all particles (standard coordinates, 4-fold symmetry), showing good representation of all views with a preference for some orientations. Plot program courtesy of Richard Henderson.

(G) Fourier shell correlation (FSC) of the structure, indicating a resolution of 21 Å at a correlation coefficient of 0.5.

this region carries KChIP2 and is intracellular while the smaller domain is the membrane-embedded portion of the channel. The positive peak is the only significant divergence of the two structures, as negative peaks (not shown) are smaller in magnitude and distributed over the entire difference map.

This topology is consistent with the mass distribution of the channel complex. Typical of Kv channel α subunits, Kv4.2* has six membrane spans (S1–S6, ~24 kDa) formed by ~225 of its 642 residues (the pore is S5–S6), flanked by intracellular N- and C-terminal domains (186 and 245 residues, respectively) that make up the bulk of the protein mass. The N terminus provides those residues known to interact with cytosolic accessory subunits including KChIPs (An et al., 2000), Frequenin (Nakamura et al., 2001; Guo et al., 2002), and Kvβs (Gulbis et al., 2000). Thus, four Kv4.2 membrane domains are predicted to have a combined molecular weight of ~96 kDa while the intracellular domain (termini of four Kv4.2 and four KChIP2 subunits) should include a total of ~310 kDa.

Identification of the smaller Kv4.2*-KChIP2 domain as the membrane portion was at first surprising because this domain in Shaker has a similar number of residues (~250) but is much larger when visualized by EM (Figure 4A; Sokolova et al., 2001). The identification can be judged correct, nonetheless, by the superimposition of the Shaker and Kv4.2*-KChIP2 structures when overlaid using the four internal columns of the hanging gondola as a guide (Figures 4A–4C). As the EM volume of the membrane domain in Kv4.2*-KChIP2 is in keeping with that expected from its mass, we suspect it is smaller than in Shaker because it is not subject to posttranslational decoration with carbohydrate. Indeed, the lower half of the membrane domain of Shaker and the top of Kv4.2*-KChIP2 are coincident (Figure 4C, top), suggesting the protein portion of the membrane domain in Shaker may be similar in volume. Good alignment of the four central columns suggests the hanging gondola in Kv4.2*-KChIP2 is like that in Shaker and shows KChIP2 incorporation to extend the platform laterally to meet four new peripheral columns. This encloses the gondola within a fenestrated rotunda with four lateral outer windows that are separated by a vestibule (and offset by 45°) from the four inner windows of the gondola (Figure 4C, bottom).

In this study, we used negative staining to enhance image contrast and obtain a reliable alignment of individual particle images. Negative staining can produce artifacts, such as flattening or uneven staining. However, agreement of important details with the previously determined Shaker structure (Sokolova et al., 2001) and successful docking of crystal structures corresponding to channel fragments (next) argue that artifacts, if present, must be small.

Discussion

To assess how incorporation of four KChIP2 molecules might create four peripheral columns and the rotunda, the arrangement of KChIP2 subunits was surmised by rendering the surface of the Kv4.2*-KChIP2 structure,

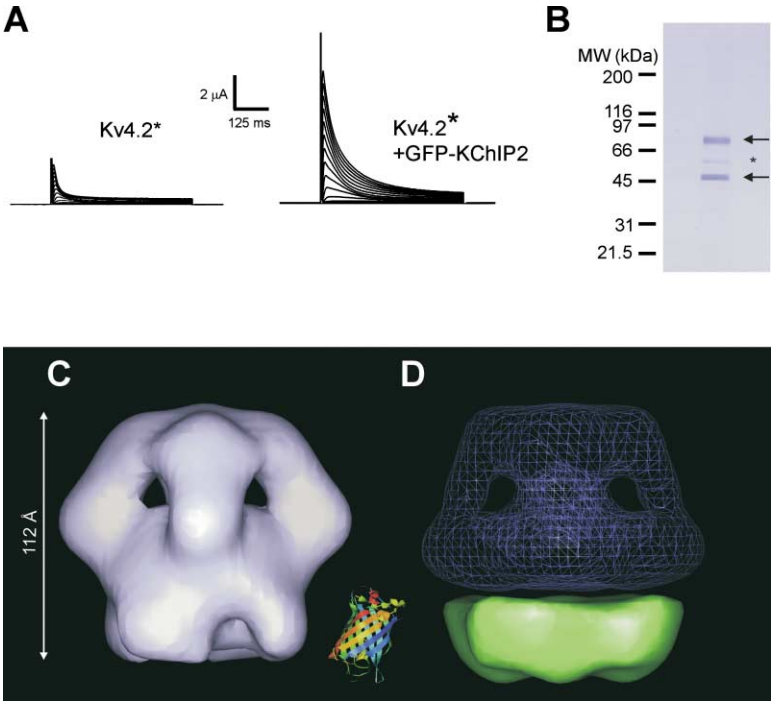

Figure 3. EM Structure of Kv4.2*-GFP-KChIP2 Identifies the Cytoplasmic Domain

(A) Current families for Kv4.2* channels and Kv4.2*-GFP-KChIP2 channels expressed in oocytes and studied by two-electrode voltage clamp show GFP-KChIP2 subunits to function like their unaltered congeners (biophysical parameters are listed in Supplemental Table S1 at http://www.neuron.org/cgi/content/full/41/4/513/DC1). Currents were evoked by steps from −100 mV to test potentials of −80 to 70 mV in 10 mV steps of 500 ms every 5 s.

(B) Purified Kv4.2*-GFP-KChIP2 channels separated by SDS-PAGE and stained with Coomassie blue to show Kv4.2* (upper arrow) and GFP-KChIP2 (lower arrow) at their predicted kDa. The band with a star is a minor (<1%), nonchannel component that is seen with anti-1D4 antibody beads, as noted (Kim et al., 2003).

(C) Side view of Kv4.2*-GFP-KChIP2 channel (pale blue), revealing a structure that is ~110 Å in height with prominent surface features. Inset is the crystal structure of eGFP (Hanson et al., 2002).

(D) The difference map of Kv4.2*-GFP-KChIP2 and Kv4.2*-KChIP2 (green) with the Kv4.2*-KChIP2 parent structure superimposed (blue mesh) reveals that new density due to inclusion of four GFP molecules is below the larger domain. This indicates that the domain carries KChIP2, and therefore, that it is in the cytosol.

superimposing the Shaker density, and considering how four molecules of the KChIP2 homolog Frequenin (Bourne et al., 2001) could be accommodated (Figure 5A). The only satisfactory docking strategy was to place the wide hydrophobic crevice of Frequenin (thought to coordinate ligand) facing toward the lateral aspect of the gondola platform—a structure formed by Kv4.2 N termini that are known to interact with NCS proteins (An et al., 2000; Bahring et al., 2001). At 21 Å resolution, it was not possible to ascertain the precise tilt of Frequenin relative to the sides of the gondola platform. Nevertheless, other Frequenin locations (for example, inside the peripheral columns) or orientations differing by more than 30° from that shown place portions of the molecule outside the Kv4.2*-KChIP2 structure or within the Shaker density and are therefore unlikely. Indeed, automated docking of Frequenin within the Kv4.2*-KChIP2 electron density map, using an exhaustive search algorithm that relied only on complementary shape and volume and excluded information about the known interaction sites between the N termini and NCS proteins, indicates the four most likely locations to be the corners of the larger domain (Supplemental Figure S3 at http://www.neuron.org/cgi/content/full/41/4/513/DC1) as we deduce based on Shaker overlay and known sites of intersubunit contact (Figure 5A).

Docking the crystal structures for T1-Kvβ2 (Gulbis et al., 2000) into Kv4.2*-KChIP2 (guided by the known

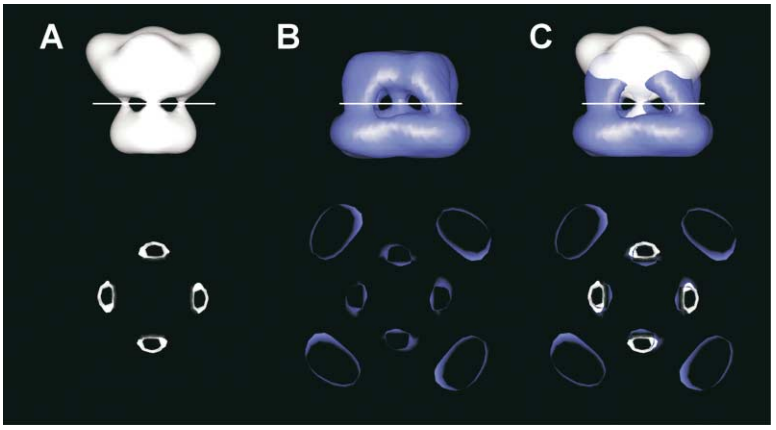

Figure 4. Shaker and Kv4.2*-KChIP2 Channels Have Similar Hanging Gondolas

(A) Shaker channel EM structure in side view (Sokolova et al., 2001) (top) and cross-section (bottom) through a plane indicated by a line in the top image show the four columns and platform of the hanging gondola that are in the cytoplasm under the membrane portion of the channel.

(B) Kv4.2*-KChIP2 channel EM structure in side (top) and cross-sectional (bottom) views equivalent to those in (A) show four internal columns around the central axis of symmetry and four peripheral columns.

(C) Superimposition of (A) and (B) shows overlap of the four central columns of the hanging gondola. The external columns are present only in the KChIP2-bearing structure. The difference in volume of the extracellular regions of the membrane domains of Shaker and Kv4.2*-KChIP2 structures is ~90 kDa assuming a protein density of 810 Da/nm^3 (Matthews, 1968). Compared to Kv4.2, Shaker has an extra mass of ~16 kDa/subunit due to glycosylation and ~4 kDa due to protein in S1–S6 region or ~80 kDa, in reasonable agreement with the measured value.

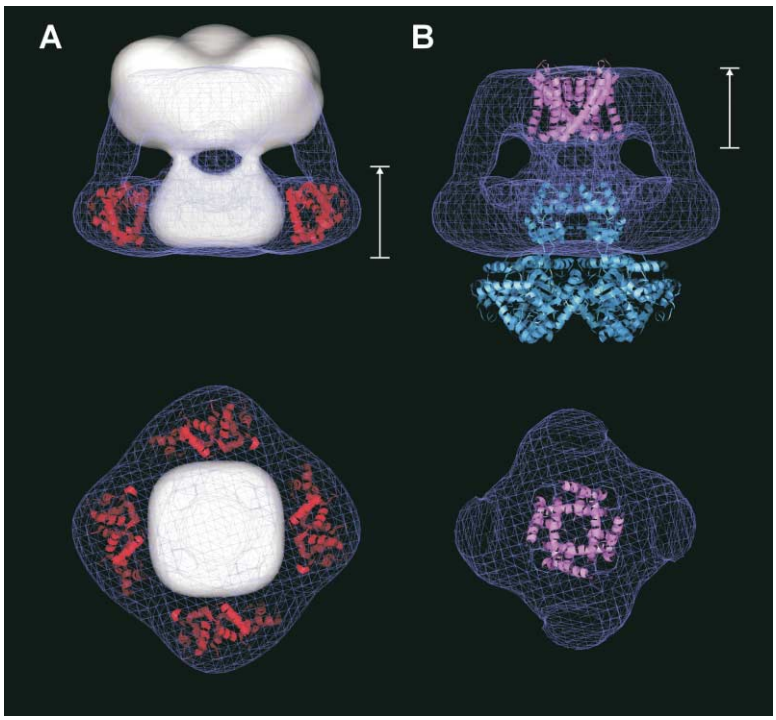

Figure 5. The Kv4.2*-KChIP2 Structure Accommodates Four NCS Monomers

(A) The Shaker channel EM structure (Sokolova et al., 2001) (white) overlaid on the Kv4.2*-KChIP2 EM structure (blue mesh) with alignment of the four central columns of the gondola from the side (top panel) and viewed from below (bottom panel) as indicated by the arrow above; this shows the Shaker membrane domain is taller, coincidence of the internal columns and windows of the gondola and ready fit of the Frequenin monomer crystal structure (Bourne et al., 2001) (red, two shown). Four Frequenin monomers (190 residues each) fit the height and width of the Kv4.2*-KChIP2 lower domain only when arranged so that the hydrophobic pocket faces the gondola platform. This is consistent with reports that KChIP2 and Frequenin bind to residues 2–40 of the Kv4.2 N terminus (An et al., 2000; Bahring et al., 2001).

(B) Crystal structures of T1-Kvβ2 (Gulbis et al., 2000) (cyan, complete octamer shown) and the KvAP (Jiang et al., 2003) pore domain (S5–S6, magenta, four shown) are overlaid on the Kv4.2*-KChIP2 EM structure (blue mesh). Viewed from the side (top panel), this composite structure shows that the Kvβ2 tetramer below the gondola platform does not overlap Frequenin and that the height of the KvAP pore is well matched to that of the Kv4.2*-KChIP2 membrane domain. The bottom panel views the membrane domain of Kv4.2*-KChIP2 from below (as indicated by the arrow top) and shows contact sites of the four internal and four peripheral columns with the domain relative to the pore.

formation of the gondola by T1) emphasizes that the height and width of the NCS protein can explain the lateral extension of the gondola platform on KChIP2 incorporation (Figure 5B). Moreover, the location of KChIP2 subunits in our structure does not overlap with the subplatform locale for the Kvβ2 subunits, suggesting that both accessory subunits might bind simultaneously. While Kv4.2 is known to interact with Kvβ family subunits (Nakahira et al., 1996), KChIP2-Kv4.2-Kvβ assemblies have not yet been described.

The crystal structure for the S1–S6 portion (223 residues) of the archeal voltage-gated potassium channel KvAP was recently determined (Jiang et al., 2003). Like Kv4.2, KvAP does not carry carbohydrate, and the height of the KvAP pore (segments S5–S6, magenta) fits well into the Kv4.2*-KChIP2 membrane domain (Figure 5B). Similarly, the pore of MthK, a calcium-sensitive potassium channel observed in the open state (Jiang et al., 2002) fits well, whereas KcsA (Zhou et al., 2001b), imaged in the closed state, is too tall (not shown). This is consistent with our expectation that purified Kv4.2*-KChIP2 complexes are in the open/inactivated state (since there is no voltage gradient across the channel). While the membrane domain can accommodate both the volume of the KvAP pore with four isolated voltage sensor (S1–S4) domains (not shown), docking the complete KvAP structure positions its S3–S4 voltage-sensing paddles below the density for the Kv4.2*-KChIP2 membrane domain (not shown), as expected due to antibody perturbation (Jiang et al., 2003).

The Kv4.2*-KChIP2 structure reveals that KChIP2 does not interact directly with the membrane domain of the channel to influence function but acts via the four internal and four external columns. While the Kv4.2 N terminus interacts with NCS proteins (An et al., 2000; Bahring et al., 2001) and mutations in the region have modest effects on channel opening and closing (gating) (Cushman et al., 2000), functional and structural studies indicate that C termini are fundamental in potassium channel gating (Goldstein et al., 2001; Jiang et al., 2002, 2003; Kuo et al., 2003; Sokolova et al., 2003); a notable example in the context of this report is triggered opening of SK potassium channels via calcium binding to the intracellular protein calmodulin that is coordinated by the α subunit C terminus just after the S6 span (Schumacher et al., 2001). Further, a central hanging gondola like that formed in Shaker channels by N-terminal T1 segments appears to be intact within the Kv4.2*-KChIP2 fenestrated rotunda. These observations lead us to speculate that in Kv4.2*-KChIP2 channels, the C termini of Kv4.2* subunits (following the S6 segment) track from the central pore to the periphery where they contribute to formation of the distal portion of the four peripheral columns; non-T1 N-terminal residues may contribute just below the membrane. The Kv4.2*-KChIP2 structure supports the idea that in vivo potassium channels are large macromolecular machines with a great deal of activity (and the majority of their protein mass) hidden below the membrane surface (Chung et al., 1991).

Experimental Procedures

Molecular Biology

Human Kv4.2 (accession number AH009258), human KChIP2 (AF199598), Kv4.2*, and GFP-KChIP2 were expressed in pRAT, as before (Kim et al., 2003). GFP-KChIP2 was made by introducing an HpaI site before the KChIP2 start codon and SalI and HpaI sites at

the 5′ and 3′ ends of eGFP (pEGFP-C1, accession number U55763, Clontech, Palo Alto, CA) with pfu-based mutagenesis to create a single ORF for eGFP-ValAsn-KChIP2. All products were verified by DNA sequencing. cRNA was synthesized, analyzed, and injected into oocytes, as before (Kim et al., 2003).

Electron Microscopy

Kv4.2*-KChIP2 and Kv4.2*-GFP-KChIP2 were purified from COS7 cells, as before (Kim et al., 2003), into a buffer containing 0.7% CHAPS, 100 mM NaCl, 40 mM KCl, 0.01 mM leupeptin/pepstatin, 1 mM EDTA, 20 mM HEPES-KOH (pH 7.4) with complete protease inhibitors (Roche) and 0.2 mg/ml of 1D4 octapeptide. Three microliters of fresh protein was placed on glow-discharged, carbon-coated copper grids, excess material was blotted with filter paper, and grids were washed with detergent-free buffer (300 mM NaCl, 40 mM KCl, 0.01 mM leupeptin/pepstatin, 1 mM PMSF, 1 mM EDTA, 20 mM HEPES-KOH [pH 7.4]) before staining with 1% uranyl acetate. Images were recorded with a Philips CM12 electron microscope at an acceleration voltage of 120 keV, magnification of 60,000× and 1.5 μm defocus. For each channel construct, 63 and 60 micrographs were scanned, respectively, on a Zeiss SCAI scanner with a 7 μm pixel size. 4 × 4 pixels were averaged to give 28 μm per pixel on the micrograph or 4.67 Å at the specimen level. For Kv4.2*-KChIP2 and Kv4.2*-GFP-KChIP2, 8314 and 5533 particles were selected, respectively, and processed as below.

Image Analysis

Image processing was performed with IMAGIC (van Heel et al., 1996), as before (Sokolova et al., 2001). Briefly, Kv4.2*-KChIP2 particles were chosen, images were band-pass filtered (the low-resolution cutoff was about 200 Å to remove any density gradients across the particle images; the high-resolution cutoff was about 12 Å to remove the least reliable portion of the data), normalized, and rotationally and translationally aligned. A reference was calculated using the aligned images and used for alignment and averaging through five iterations. Aligned images were subjected to multivariate statistical analysis (MSA) for classification. The best classes were used for multireference alignment (MRA) to further refine the orientations of each particle. Four additional cycles of MRA, MSA, and classification were performed. Four of the final classes that show approximate 4-fold symmetry are shown in Supplemental Figure S1 at http://www.neuron.org/cgi/content/full/41/4/513/DC1. Using angular reconstitution, the relative orientations of the final classes were determined and used to calculate a 3D reconstruction with imposed 4-fold symmetry. Reprojections were used for iterative MRA until a stable structure was obtained. This initial set of Euler angles was used for the starting conditions for FREALIGN (Grigorieff, 1998), a program that refines the structure by correcting for the CTF and minimizing phase residuals between each particle and the reference structure. Data from 5037 additional images (obtained from a complex of KChIP2 and a Kv4.2* truncation variant lacking the last 98 amino acids) were used for further refinement of the reference structure and then removed to produce a final Kv4.2*-KChIP2 structure. For both Kv4.2*-KChIP2 and Kv4.2*-GFP-KChIP2 structures, refinement in FREALIGN was repeated for 15 iterations until a stable structure was obtained. The final structures contained 8164 and 4449 particles, respectively.

To calculate a difference map between the structures of Kv4.2*-KChIP2 and Kv4.2*-GFP-KChIP2, the structures were aligned by maximizing a correlation coefficient determined within the bounds of the Kv4.2*-KChIP2 structure while constraining the directions of the 4-fold symmetry axes to be parallel or antiparallel, yielding values of 0.54 and 0.39, respectively. The parallel orientation (shown in Figure 3C) is thus most consistent with the data. Difference maps were calculated by a standard strategy with maps scaled using least-squares minimization of the structure factors in each resolution zone (zonal scaling).

Visualization

Crystal structures and density maps for Shaker, Kv4.2*-KChIP2, and Kv4.2*-GFP-KChIP2 were visualized with Chimera, a graphics package from the Computer Graphics Laboratory, UCSF (http://www.cgl.ucsf.edu/chimera) (Huang et al., 1996). Assuming a density of 810 Da/nm^3 (Matthews, 1968), the weight included in the contoured volumes for Kv4.2*-KChIP2 and Kv4.2*-GFP-KChIP2 in Figures 2 and 3C are about 390 kDa and 520 kDa, respectively, in reasonable agreement with their expected weights of about 410 kDa and 520 kDa, respectively. Crystal structures were docked manually and confirmed by an automated method (Supplemental Figure S3 at http://www.neuron.org/cgi/content/full/41/4/513/DC1).

Acknowledgments

This work was supported by grants from the NIH to S.A.N.G. (a Doris Duke Distinguished Clinical Scholar) and N.G. L.A.K. is in the Medical Scientist Training Program (GM07205). J.F. was supported by a fellowship from the Max Kade Foundation. We thank G. Abbott, D. Goldstein, I. O'Kelly, and C. Miller for thought-provoking discourse.

Received: November 13, 2003
Revised: January 16, 2004
Accepted: January 22, 2004
Published: February 18, 2004

References

Abbott, G.W., and Goldstein, S.A.N. (1998). A superfamily of small potassium channel subunits: form and function of the MinK-related peptides (MiRPs). Q. Rev. Biophys. *31*, 357–398.

An, W.F., Bowlby, M.R., Bett, M., Cao, J., Ling, H.P., Mendoza, G., Hinson, J.W., Mattsson, K.I., Strassle, B.W., Trimmer, J.S., and Rhodes, K.J. (2000). Modulation of A-type potassium channels by a family of calcium sensors. Nature *403*, 553–556.

Bahring, R., Dannenberg, J., Peters, H.C., Leicher, T., Pongs, O., and Isbrandt, D. (2001). Conserved Kv4 N-terminal domain critical for effects of Kv channel-interacting protein 2.2 on channel expression and gating. J. Biol. Chem. *276*, 23888–23894.

Bourne, Y., Dannenberg, J., Pollmann, V., Marchot, P., and Pongs, O. (2001). Immunocytochemical localization and crystal structure of human frequenin (neuronal calcium sensor 1). J. Biol. Chem. *276*, 11949–11955.

Chung, S.K., Reinhart, P.H., Martin, B.L., Brautigan, D., and Levitan, I.B. (1991). Protein kinase activity closely associated with a reconstituted calcium-activated potassium channel. Science *253*, 560–562.

Cushman, S.J., Nanao, M.H., Jahng, A.W., DeRubeis, D., Choe, S., and Pfaffinger, P.J. (2000). Voltage dependent activation of potassium channels is coupled to T1 domain structure. Nat. Struct. Biol. *7*, 403–407.

Goldstein, S.A.N., Bockenhauer, D., O'Kelly, I., and Zilberberg, N. (2001). Potassium leak channels and the KCNK family of two-P-domain subunits. Nat. Rev. Neurosci. *2*, 175–184.

Grigorieff, N. (1998). Three-dimensional structure of bovine NADH: ubiquinone oxidoreductase (complex I) at 22 Å in ice. J. Mol. Biol. *277*, 1033–1046.

Gulbis, J.M., Mann, S., and MacKinnon, R. (1999). Structure of a voltage-dependent K^+ channel beta subunit. Cell *97*, 943–952.

Gulbis, J.M., Zhou, M., Mann, S., and MacKinnon, R. (2000). Structure of the cytoplasmic beta subunit—T1 assembly of voltage-dependent K^+ channels. Science *289*, 123–127.

Guo, W., Malin, S.A., Johns, D.C., Jeromin, A., and Nerbonne, J.M. (2002). Modulation of Kv4-encoded K^+ currents in the mammalian myocardium by neuronal calcium sensor-1. J. Biol. Chem. *277*, 26436–26443.

Hanson, G.T., McAnaney, T.B., Park, E.S., Rendell, M.E., Yarbrough, D.K., Chu, S., Xi, L., Boxer, S.G., Montrose, M.H., and Remington, S.J. (2002). Green fluorescent protein variants as ratiometric dual emission pH sensors. 1. Structural characterization and preliminary application. Biochemistry *41*, 15477–15488.

Huang, C.C., Couch, G.S., Pettersen, E.F., and Ferrin, T.E. (1996). Chimera: An Extensible Molecular Modeling Application Constructed Using Standard Components. Pacific Symposium on Biocomputing *1*, 724.

Jiang, Y.X., Lee, A., Chen, J., Cadene, M., Chait, B.T., and MacKin-

non, R. (2002). Crystal structure and mechanism of a calcium-gated potassium channel. Nature *417*, 515–522.

Jiang, Y.X., Lee, A., Chen, J.Y., Ruta, V., Cadene, M., Chait, B.T., and MacKinnon, R. (2003). X-ray structure of a voltage-dependent K^+ channel. Nature *423*, 33–41.

Kim, L.A., Furst, J., Butler, M., Xu, S., Grigorieff, N., and Goldstein, S.A.N. (2003). I_{to} channels are octameric complexes with four subunits of each Kv4.2 and K^+ channel-interacting protein 2 (KChIP2). J. Biol. Chem., in press. Published online November 17, 2003. 10.1074/jbc.M311332200

Kobertz, W.R., Williams, C., and Miller, C. (2000). Hanging gondola structure of the T1 domain in a voltage-gated K^+ channel. Biochemistry *39*, 10347–10352.

Kreusch, A., Pfaffinger, P.J., Stevens, C.F., and Choe, S. (1998). Crystal structure of the tetramerization domain of the Shaker potassium channel. Nature *392*, 945–948.

Kuo, H.C., Cheng, C.F., Clark, R.B., Lin, J.J., Lin, J.L., Hoshijima, M., Nguyen-Tran, V.T., Gu, Y., Ikeda, Y., Chu, P.H., et al. (2001). A defect in the Kv channel-interacting protein 2 (KChIP2) gene leads to a complete loss of I_{to} and confers susceptibility to ventricular tachycardia. Cell *107*, 801–813.

Kuo, A., Gulbis, J.M., Antcliff, J.F., Rahman, T., Lowe, E.D., Zimmer, J., Cuthbertson, J., Ashcroft, F.M., Ezaki, T., and Doyle, D.A. (2003). Crystal structure of the potassium channel KirBac1.1 in the closed state. Science *300*, 1922–1926.

Matthews, B.W. (1968). Solvent content of protein crystals. J. Mol. Biol. *33*, 491–497.

Nakahira, K., Shi, G., Rhodes, K.J., and Trimmer, J.S. (1996). Selective interaction of voltage-gated K^+ channel beta-subunits with alpha-subunits. J. Biol. Chem. *271*, 7084–7089.

Nakamura, T.Y., Pountney, D.J., Ozaita, A., Nandi, S., Ueda, S., Rudy, B., and Coetzee, W.A. (2001). A role for frequenin, a Ca^{2+}-binding protein, as a regulator of Kv4 K^+-currents. Proc. Natl. Acad. Sci. USA *98*, 12808–12813.

Orlova, E.V., Papakosta, M., Booy, F.P., van Heel, M., and Dolly, J.O. (2003). Voltage-gated K^+ channel from mammalian brain: 3D structure at 18Å of the complete $\alpha 4\beta 4$ complex. J. Mol. Biol. *326*, 1005–1012.

Rosati, B., Pan, Z., Lypen, S., Wang, H.S., Cohen, I., Dixon, J.E., and McKinnon, D. (2001). Regulation of KChIP2 potassium channel beta subunit gene expression underlies the gradient of transient outward current in canine and human ventricle. J. Physiol. *533*, 119–125.

Schumacher, M.A., Rivard, A.F., Bachinger, H.P., and Adelman, J.P. (2001). Structure of the gating domain of a $Ca2^+$-activated K^+ channel complexed with $Ca2^+$/calmodulin. Nature *410*, 1120–1124.

Shibata, R., Misonou, H., Campomanes, C.R., Anderson, A.E., Schrader, L.A., Doliveira, L.C., Carroll, K.I., Sweatt, J.D., Rhodes, K.J., and Trimmer, J.S. (2003). A fundamental role for KChIPs in determining the molecular properties and trafficking of Kv4.2 potassium channels. J. Biol. Chem. *278*, 36445–36454.

Sokolova, O., Kolmakova-Partensky, L., and Grigorieff, N. (2001). Three-dimensional structure of a voltage-gated potassium channel at 2.5 nm resolution. Structure *9*, 215–220.

Sokolova, O., Accardi, A., Gutierrez, D., Lau, A., Rigney, M., and Grigorieff, N. (2003). Conformational changes in the C terminus of Shaker K+ channel bound to the rat Kvbeta2-subunit. Proc. Natl. Acad. Sci. USA *100*, 12607–12612.

Takimoto, K., Yang, E.K., and Conforti, L. (2002). Palmitoylation of KChIP splicing variants is required for efficient cell surface expression of Kv4.3 channels. J. Biol. Chem. *277*, 26904–26911.

van Heel, M., Harauz, G., Orlova, E.V., Schmidt, R., and Schatz, M. (1996). A new generation of the IMAGIC image processing system. J. Struct. Biol. *116*, 17–24.

Zhou, M., Morais-Cabral, J.H., Mann, S., and MacKinnon, R. (2001a). Potassium channel receptor site for the inactivation gate and quaternary amine inhibitors. Nature *411*, 657–661.

Zhou, Y., Morais-Cabral, J.H., Kaufman, A., and MacKinnon, R. (2001b). Chemistry of ion coordination and hydration revealed by a K^+ channel-Fab complex at 2.0 Å resolution. Nature *414*, 43–48.